Fatigue Crack Growth Properties of a GLARE3-5/4 Fiber/Metal Laminate*

Tohru TAKAMATSU*1, Takashi MATSUMURA*2, Norio OGURA*3,
Toshiyuki SHIMOKAWA*4, and Yoshiaki KAKUTA*4

ABSTRACT

The objective of this study is to investigate the properties of fatigue crack growth in GLARE3-5/4 fiber/metal laminate and the validity of methods for analyzing the fatigue crack growth of fiber/metal laminates. GLARE3-5/4 consists of five thin sheets of 2024-T3 aluminum alloy and four layers of (0/90) glass/epoxy. Centrally notched specimens were fatigue tested under constant amplitude loading and crack length was measured using the DC potential-drop method. The size of the delamination produced between aluminum alloy sheets and fiber-adhesive layers was measured from ultrasonic C-scan pictures taken around the fatigue crack. The test results indicated the features of fatigue crack growth in GLARE3-5/4. The validity of two methods for analyzing the fatigue crack growth of fiber/metal laminates is discussed based on the test results.

Keywords: fiber/metal laminate, GLARE, fatigue, crack growth, variability, stress intensity factor, fiber bridging, delamination, analytical method

概　要

本研究の目的は，ファイバーメタル積層材料 GLARE3-5/4 における疲労き裂進展特性を調べるとともに，ファイバーメタル積層材料におけるき裂進展を解析する方法の有効性について調べることである。GLARE3-5/4 は５枚のアルミニウム合金薄板とガラス／エポキシ４層からなる。中央部に切欠きを有する試験片に対して一定振幅荷重下の疲労試験を行い，き裂長さをDCポテンシャルドロップ法により測定した。また，アルミニウム合金シートと繊維・接着層との層間剥離の大きさは，き裂周りを超音波C-スキャンにより撮影した写真から計測した。試験結果は，GLARE3-5/4 における疲労き裂進展の特徴を明らかにした。また試験結果に基づき，ファイバーメタル積層材料におけるき裂進展を解析する２種類の方法について，その有効性を検討した。

INTRODUCTION

Fiber/metal laminates were originally developed by the Delft University of Technology at the beginning of 1980 [1]. Each of the laminates is alternatively laid up by a thin sheet of a high-strength aluminum alloy and a layer of fiber/epoxy as shown in Figure 1. These materials are divided into three groups: ARALL, GLARE, and CARALL due to the different fiber-adhesive layers used, i.e., aramid fibers, glass fibers, and carbon fibers respectively. Each one of them has excellent fatigue resistance and is a promising candidate for the structural materials of advanced aircraft.

* Received 31, August, 1998

*1 Guest Researcher of NAL, University of Electro-Communications.
*2 University of Electro-Communications.
*3 Matsushita Communication Industrial Co., Ltd.
*4 Structures division, National Aerospace laboratory.

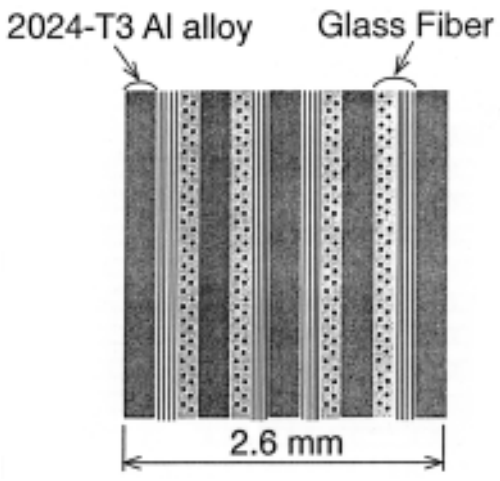

Fig. 1 Schematic view in the thickness direction of a GLARE3-5/4.

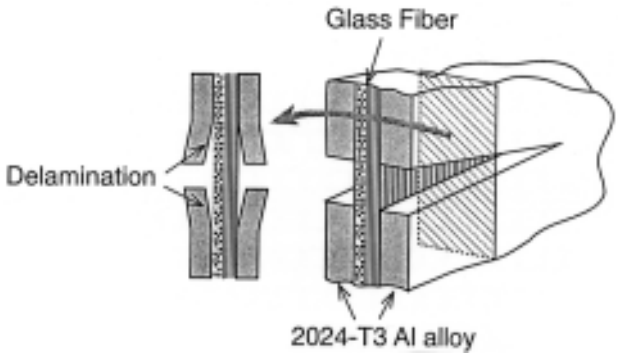

Fig. 2 Fiber bridging effect in a fiber/metal laminate.

Fatigue crack growth has been investigated for ARALLs [2],[3],[6]-[11], GLAREs [2]-[6], and CARALLs [12]. The test results confirmed that the relationship between the crack growth rate, da/dN, and stress intensity factor range, ΔK, on the assumption of a monolithic material did not agree with that obtained for a monolithic aluminum alloy. This disagreement was explained by a fiber-bridging effect as illustrated in Figure 2 that controls crack opening. Namely, a fatigue crack propagates in aluminum alloy sheets; however, fibers are not easily broken, and unbroken fibers prevent the crack from opening. Therefore, da/dN does not become as high as that in a monolithic aluminum alloy, even though the crack grows longer.

Marissen [8] derived an expression for a stress intensity factor for a centrally cracked specimen of an ARALL, taking account of the effects of fiber bridging and delamination between a metallic sheet and a fiber-adhesive layer. Toi [5] proposed a simple model to analyze crack growth in GLAREs using a modified factor obtained from the da/dN versus ΔK relationships of GLAREs and 2024-T3 aluminum alloy. However, the validity of Marissen's expression for a stress intensity factor or Toi's model has not generally been confirmed yet. Moreover, no example of the variation of fatigue crack growth can be found for fiber/metal laminates, though this is a very important property in evaluating the reliability of these materials. The present study selected a GLARE3-5/4 fiber/metal laminate and used centrally notched specimens for fatigue crack growth tests. The crack growth properties of this material have not been investigated to date. The purposes of this study are as follows: (1) The scatter in crack growth is investigated and compared with that of a 2024-T3 aluminum alloy obtained in the previous studies [13],[14]. (2) The validity of Toi's model is examined for the da/dN versus ΔK relationship for the GLARE3-5/4. (3) The da/dN versus ΔK relationship is analyzed by using Marissen's formula for a stress intensity factor and compared with that for a 2024-T3 aluminum alloy.

EXPERIMENTAL PROCEDURES

Materials and Specimens

Figure 1 depicts a schematic view in the thickness direction of the tested GLARE3-5/4. GLARE3-5/4 consists of five sheets of 2024-T3 aluminum alloy (0.3 mm thick) and four layers of glass/epoxy (0.28 mm thick) with a stacking sequence of (0/90). The total thickness is 2.6 mm and thickest among the GLAREs manufactured to date.

Table 1 indicates the mechanical properties of the GLARE3-5/4. Figure 3(a) illustrates the configuration of centrally notched specimens, 350 mm long, 70 mm wide, notch length of 3.0 mm, and notch root radius of 0.35 mm. In order to measure crack growth of the 2024-T3 aluminum alloy which composed GLARE3-5/4, a single-layer specimen of the alumi-

Table 1 Mechanical properties of the GLARE3-5/4 tested.

Material	$\sigma_{0.2}$ MPa	σ_B MPa	E GPa	Poisson's ratio ν	δ %
GLARE3-5/4	323	764	58	0.28	5

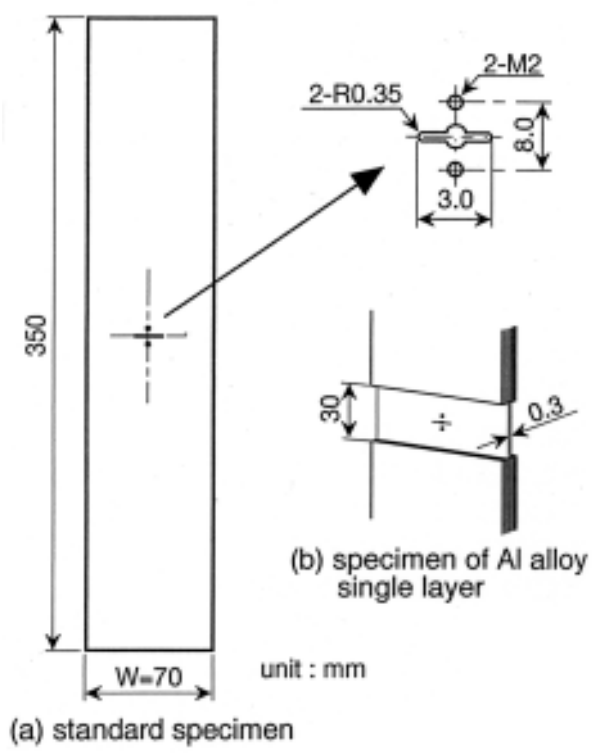

Fig. 3 Specimen configurations.

num alloy (0.3 mm thickness) as shown in Figure 3(b) was also machined from a GLARE specimen.

Fatigue Testing

Fatigue tests were performed at room temperature by using a servo-hydraulic testing machine under constant amplitude loading with sinusoidal waves of frequency 5 Hz and stress ratio $R = 0.05$. The nominal maximum stress σ_{max} was chosen at three levels: 110, 147, and 196 MPa.

Figure 4 indicates a testing and measuring system developed in previous studies [13],[14]. The crack length was measured by using the DC electrical potential method. A personal computer controlled the testing machine and automatically measured the change in electrical potential with increase in crack length. The constant DC current of 13 amperes was applied to the surface aluminum alloy sheet. Fatigue testing was automatically stopped at a constant interval of load cycles. The electrical potential between two terminals on both sides of the notch was measured and converted into the equivalent value of crack length by referring to a calibration curve obtained in advance.

TEST RESULTS AND DISCUSSION

Variation of Crack Growth Lives

Fatigue tests revealed that the crack propagated in the aluminum alloy sheets and did not show unstable fracture even when the crack length was almost equal to the specimen width. In order to know how the crack propagates in the internal sheet of the aluminum alloy, the specimen in the vicinity of the crack tip was machined gradually using an end mill tool. The difference in crack lengths between the surface sheets and the center sheet was found

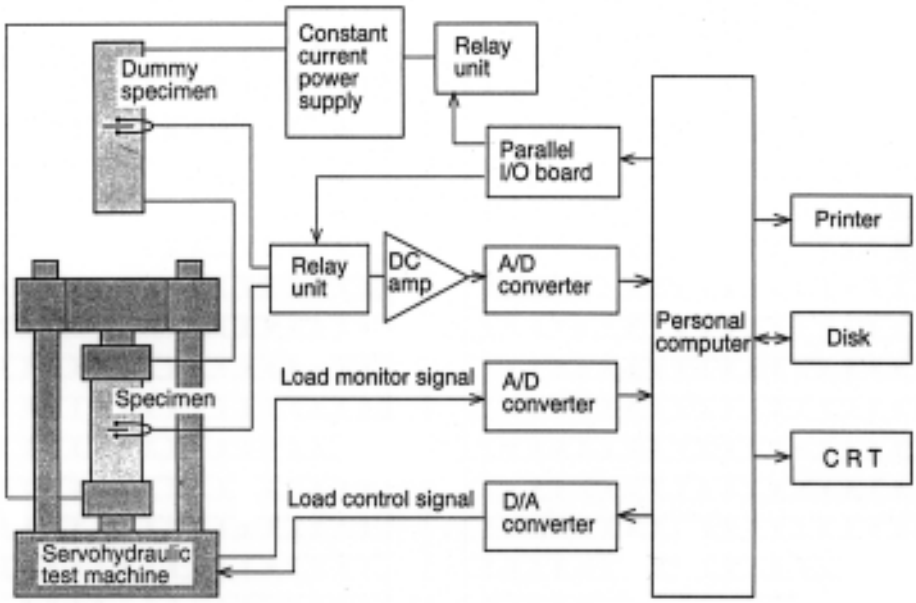

Fig. 4 Load control and crack measuring system using the DC potential drop method.

to be about 8 % in the case of a short crack, and about 2 % in the case of a long crack. It was also found that fibers hardly broke as reported by Toi [5].

Figures 5(a) and (b) show the relationships between half-crack length and number of load cycles, i.e., a—N curves. Figure 5(a) presents the result for the GLARE3-5/4 using 11 specimens at a maximum stress of 110 MPa, assuming the number of cycles to be zero at 2.5 mm crack length. Figure 5(b) presents the result for monolithic 2024-T3 aluminum alloy using 18 specimens at a maximum stress of 52 MPa obtained in the previous studies [13],[14]. Crack length was measured at intervals of 0.1 mm in both Figures 5(a) and (b). The specimen of the 2024-T3 aluminum alloy was 3.0 mm thick and had a notch of 14.0 mm long; other dimensions were the same as those of the GLARE3-5/4 in Figure 3. The difference between a—N curves for both materials is clear, and the a—N curves of the GLARE3-5/4 are approximately straight.

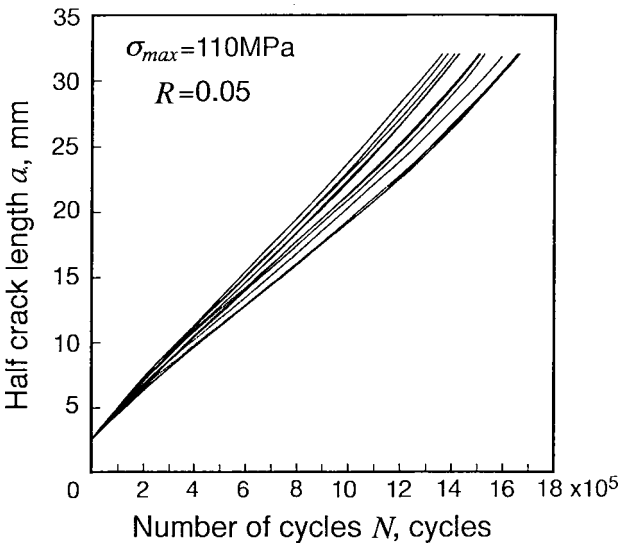

Fig. 5(a) Relationships between half-crack length and number of load cycles of 11 specimens of GLARE3-5/4 under constant amplitude loading of σ_{max} = 110 MPa and stress ratio of 0.05.

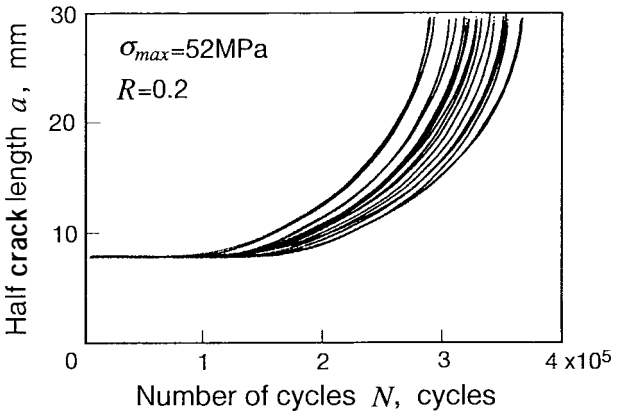

Fig. 5(b) Relationships between half-crack length and number of load cycles of 18 specimens of 2024-T3 aluminum alloy under constant amplitude loading of σ_{max} = 52 MPa and stress ratio of 0.2

The coefficient of variation of the number of cycles for a crack to grow from an initial length a_1 to an arbitrary length a_2 was calculated from the obtained data. Figures 6(a) and (b) show the relationships between the coefficient of variation, η_N, and arbitrary length, a_2, for the GLARE3-5/4 and 2024-T3 aluminum alloy respectively. The initial half-crack

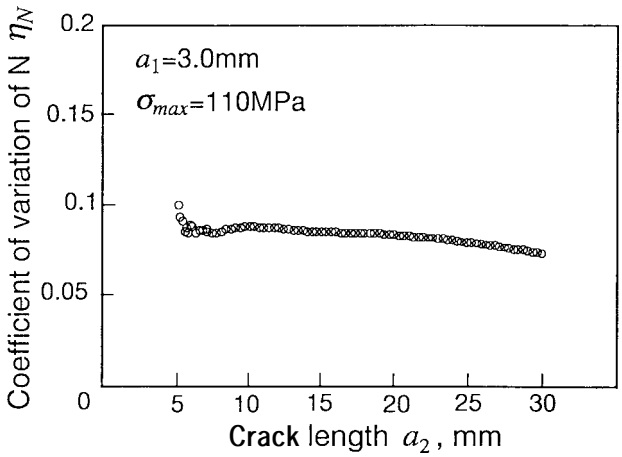

(a) GLARE3-5/4

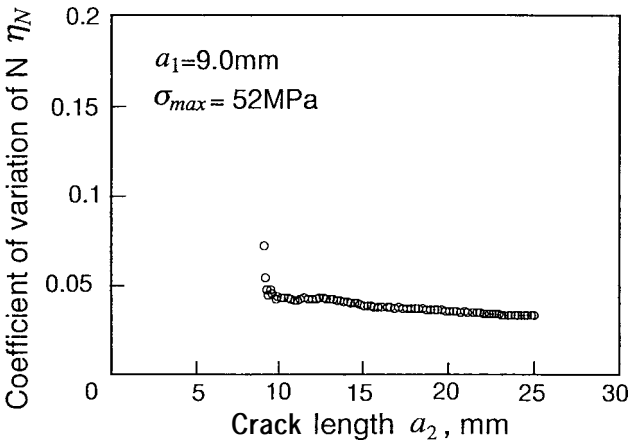

(b) 2024-T3 aluminum alloy

Fig. 6 Coefficient of variation of load cycles for a crack to grow from initial length a_1 to arbitrary length a_2.

length a_1 was 3 mm for the GLARE3-5/4 and was 9 mm for the 2024-T3 aluminum alloy. The value of η_N in the region of short crack length is somewhat large and drops stepwise, then decreases slightly as the crack length increases for both materials. The value of η_N in its slowly decreasing region is 0.08～0.09 for the GLARE3-5/4, and is 0.03～0.04 for the 2024-T3 aluminum alloy. In another study[15] of 2024-T3 aluminum alloy, η_N was 0.04～0.07. Therefore, the value of η_N for the GLARE3-5/4 in this study is about twice that for the monolithic 2024-T3 aluminum alloy.

Relationship Between Crack Growth Rate and Stress Intensity Factor Range

Figure 7 presents the a—N relationship for a single sheet specimen of aluminum alloy (0.3 mm thick) in Figure 3(b), machined from a GLARE specimen. A fatigue test was conducted at the maximum stress of 47 MPa with $R = 0.05$. The crack length was measured using a traveling microscope at intervals of about 0.1 mm.

Figure 8 shows the da/dN—ΔK data plotted on a double-log scale obtained from the a—N relationship in Figure 7. The stress intensity factor range ΔK was calculated from the following equation:

$$\Delta K = \Delta\sigma\sqrt{\pi a}\sqrt{\sec\left(\frac{\pi a}{W}\right)} \qquad (1)$$

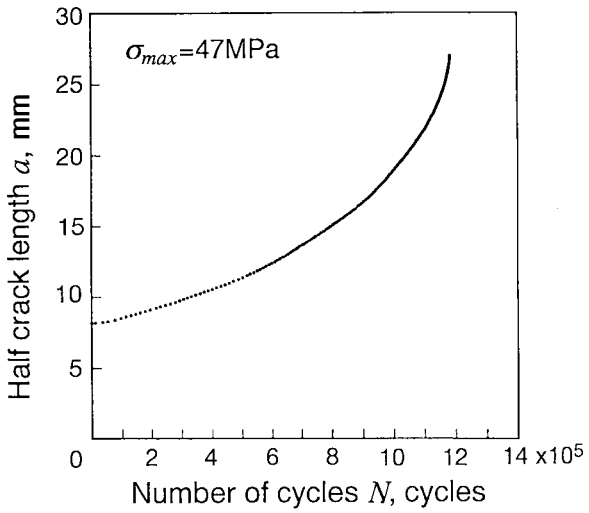

Fig. 7 Relationship between half-crack length and number of load cycles in a single sheet specimen of 2024-T3 aluminum alloy machined from a GLARE3-5/4 specimen.

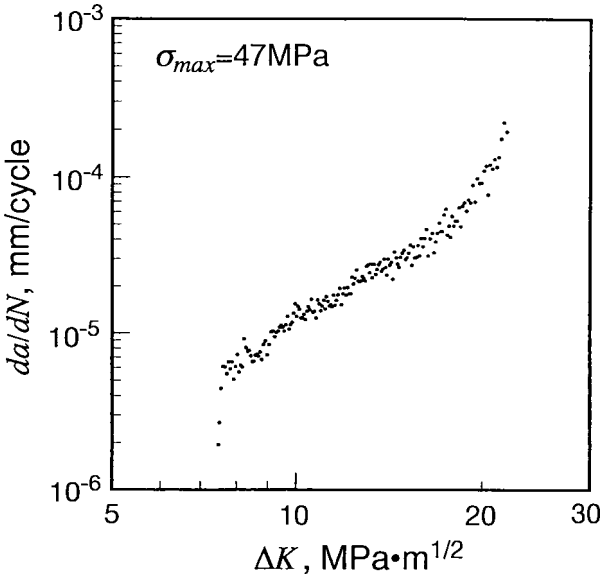

Fig. 8 Relationship between da/dN and ΔK in a single sheet specimen of 2024-T3 aluminum alloy machined from a GLARE3-5/4 specimen.

where W is the specimen width and a the half crack length.

Since the da/dN—ΔK relationship is almost straight in the range except for the vicinity of both tail regions of this data, the following Paris-Erdogan's law is applicable:

$$\frac{da}{dN} = C(\Delta K)^m \qquad (2)$$

where $m = 2.50$ and $\log C = -7.43$. This range is considered from $\Delta K = 8$ MPa•m$^{1/2}$ to 80 MPa•m$^{1/2}$.

Figure 9 indicates the da/dN—ΔK relationship obtained from an a—N curve that was arbitrarily chosen from the data of 11 specimens in Figure 5(a). However, ΔK was a nominal ΔK value and was calculated using Equation (1) assuming a monolithic material. The $da/dN - \Delta K$ relationship for the GLARE3-5/4 is different from that for a monolithic material and da/dN shows only a slight increase even though ΔK becomes large. In addition, the tendency of the $da/dN - \Delta K$ relationship varies from decreasing to increasing at a certain ΔK as the crack length increases. The decreasing tendency of da/dN in Region I in Figure 9 was mainly attributed to a bridging effect by unbroken fibers as mentioned before, and the increasing tendency of da/dN in Region II is caused by a reduction of the bridging effect generated by the extension of delamination.

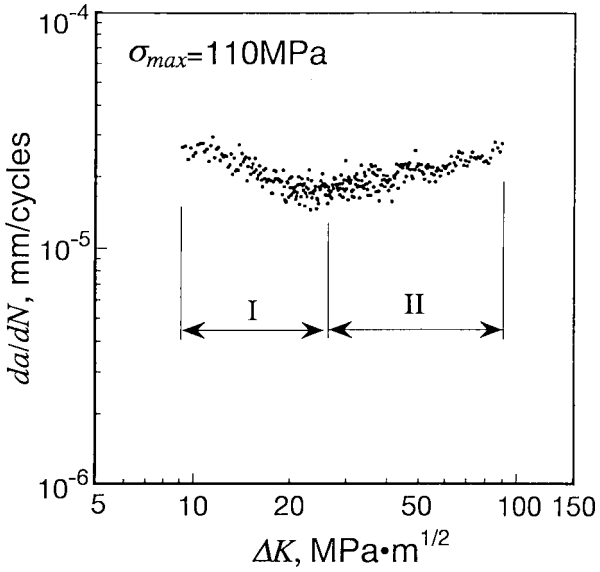

Fig. 9 Relationship between da/dN and ΔK in the GLARE3-5/4 under constant amplitude loading of σ_{max} = 110 MPa.

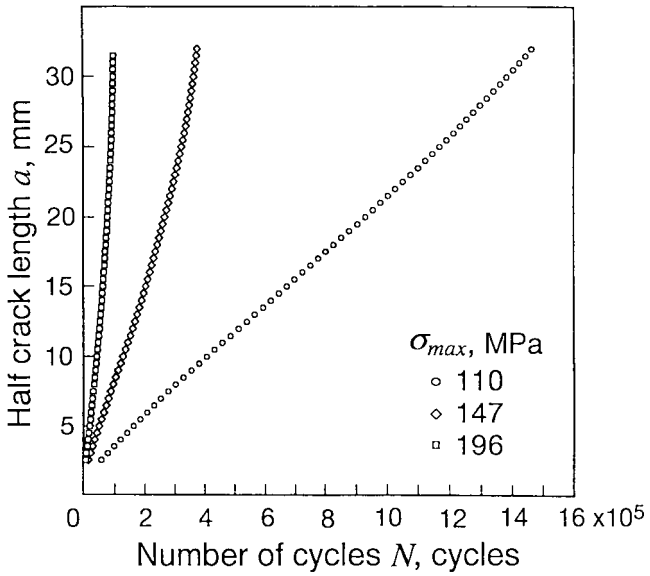

Fig. 10 Influence of the maximum stress level on the relationship between half-crack length and number of load cycles in the GLARE 3-5/4.

Figure 10 presents a—N curves obtained by the fatigue tests at the maximum stress of σ_{max} = 110, 147, and 196 MPa. The data were plotted at intervals of 0.5 mm. Figure 11 indicates the da/dN—ΔK relationships obtained from the a—N curves in Figure 10. This figure shows the averaged relationship for a single sheet specimen of the aluminum alloy also obtained from the data in Figure 8. The test results confirmed that (1) the da/dN—ΔK relationships of the GLARE3-5/4 depend on σ_{max} and become large as σ_{max} increases, and (2) a fatigue crack propagates stably up to a fairly large ΔK in contrast with the monolithic aluminum alloy specimen. The arrows in the results for the GLARE3-5/4 indicate the borderline between Regions I and II as shown in Figure 9. However, because the da/dN—ΔK relationship at σ_{max} = 196 MPa increases as a whole, the arrow in this case shows the position where the rate of increase of da/dN became large. The values of ΔK and the crack length at a boundary ΔK were obtained as follows: 25 MPa•m$^{1/2}$ and 14.5 mm at σ_{max} = 110 MPa, 29 MPa•m$^{1/2}$ and 11.9 mm at σ_{max} = 147 MPa, 35 MPa•m$^{1/2}$ and 9.8 mm at σ_{max} = 196 MPa. Consequently, the change from Region I to Region II occurred at a shorter crack length as the maximum stress increased. In addition, the rate of increase of da/dN in Region II becomes larger as the maximum stress increases, and the increase in da/dN for the

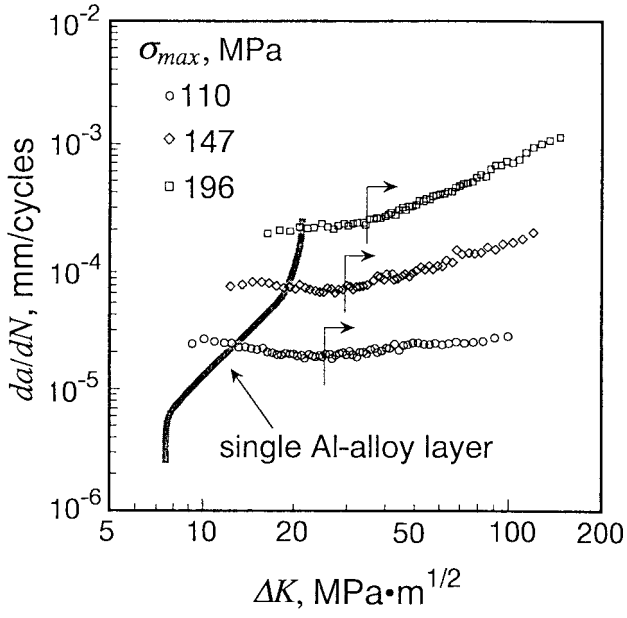

Fig. 11 Effect of the maximum stress level on the relationship between da/dN and ΔK in the GLARE3-5/4.

GLARE3-5/4 is apparently lower than that for a single-sheet specimen of the aluminum alloy.

Applicability of Toi's Model

Toi[5] indicated that the da/dN—ΔK relationships for a GLARE modified by a factor β_{fb} were independent of the maximum stress and agreed with the relationship obtained for an aluminum alloy. Toi's

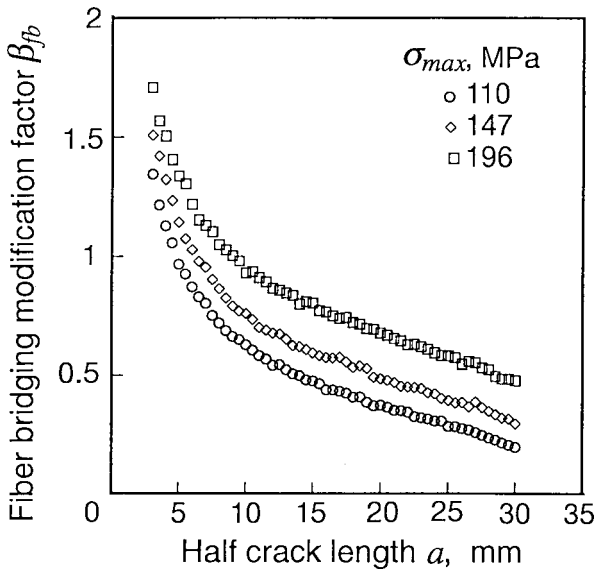

Fig. 12 Influence of the maximum stress level on the relationship between Toi's modification factor and half crack length.

model was based on the results of fatigue tests using centrally cracked specimens of GLARE 2 (1.12 mm thick) and GLARE 3 (1.62 mm thick). The modified factor β_{fb} was defined as

$$\beta_{fb} = \frac{\Delta K_{metal}}{\Delta K_{lam}} \tag{3}$$

where ΔK_{metal} was obtained from the monolithic aluminum alloy, and ΔK_{lam} from the GLARE, provided that da/dN was equal.

The β_{fb}—a relationships in Figure 12 were obtained from the da/dN—ΔK relationships in Figure 11 and Paris-Erdogan's relationship for the single-sheet specimen of the aluminum alloy in Figure 8. The β_{fb}—a relationships are confirmed to depend on σ_{max}. The β_{fb}—a relationships should be independent of σ_{max} in order that the da/dN—ΔK relationships modified by β_{fb} are independent of σ_{max}. Therefore, Toi's model is not applicable to the test results for the GLARE3-5/4 obtained in this study. However, if the dependency of σ_{max} on the da/dN—ΔK relationship can be expressed by a simple equation, Toi's model for GLARE3-5/4 will become applicable. Toi's model needs to be studied further.

Applicability of Marissen's Formula for Stress Intensity Factor

Marissen[8] derived a numerical formula for the stress intensity factor, K_{fin}, for a centrally cracked specimen of an ARALL by considering the effects of fiber bridging and delamination. His formula used the following three assumptions. (1) Cracks propagate in aluminum alloy sheets only. (2) Fibers do not break. (3) The delamination shape around a crack is an ellipse.

K_{fin} is obtained as the sum of K_{Al} with respect to the delamination size and K_{ad} related to the shear deformation of an adhesive. This is expressed as follows:

$$K_{fin} = K_{Al} + K_{ad}\,, \tag{4}$$

$$K_{Al} = C_d\,(\sigma_{Al} - \sigma_{Al,0})\,\sqrt{\pi a}\,, \tag{5}$$

$$K_{ad} = C_s\,C_{ad,d}\,(\sigma_{Al} - \sigma_{Al,0})\,\sqrt{h \cdot \tanh\left(\frac{\pi a}{h}\right)}\,, \tag{6}$$

where σ_{Al} is the stress in aluminum alloy sheets, $\sigma_{Al,0}$ is the stress with respect to residual stress $\sigma_{r,Al}$ of the aluminum alloy sheets, and C_d, C_s, $C_{ad,d}$, and h are given as a function of the relationship between the delamination size and crack length, and an elastic characteristic of the aluminum alloy, glass fibers, and adhesive:

$$\sigma_{Al,0} = -\frac{2}{\pi}\cos^{-1}\left(\frac{\sin\frac{\pi s}{W}}{\sin\frac{\pi a}{W}}\right)\sigma_{r,Al} \tag{7}$$

$$C_d = \frac{C_{fw1}}{1 + \frac{4}{\pi}\,C_{fw2}C_{b/a}\frac{\sqrt{a^2 - s^2}}{b_s}\,\frac{F_{ar}}{F_{la}}\cos^{-1}\left\{\frac{\sin\frac{\pi s}{W}}{\sin\frac{\pi a}{W}}\right\}} \tag{8}$$

$$C_{fw1} = \left\{1 - 0.1\left(\frac{a}{W}\right)^2 + 0.96\left(\frac{a}{W}\right)^4\right\}\sqrt{\sec\frac{\pi a}{W}} \tag{9}$$

$$C_{fw2} = -0.07 - 1.07\left(\frac{a}{W}\right) + 0.68\left(\frac{a}{W}\right)^2 - 0.72\left(\frac{a}{W}\right)^3 + 0.32\left(\frac{a}{W}\right)^4 - 0.54\left(\frac{W}{a}\right)\ln\left(1 - \frac{2a}{W}\right) \tag{10}$$

$$C_{b/a} = \frac{5}{3\left(1 + \frac{b_s}{\sqrt{a^2 - s^2}}\right)} - \frac{2}{3\left(1 + \frac{b_s}{\sqrt{a^2 - s^2}}\right)^2} \tag{11}$$

$$F_{la} = t_{la} E_{la}, \quad F_{gl} = t_{gl} E_{gl} \tag{12}$$

$$C_s = \frac{\cos^{-1}\left(1 - \dfrac{\pi h - \pi hs/a}{\pi h + 8a - 8s}\right)}{\cos^{-1}\left(1 - \dfrac{\pi h}{\pi h + 8a}\right)} C_{b/a} \tag{13}$$

$$\left.\begin{aligned} C_{ad,d} &= \frac{\sigma_{br}}{\sigma_{la} - \sigma_{la,0}} + \left(1 - \frac{\sigma_{br}}{\sigma_{la} - \sigma_{la,0}}\right) \ln\left(1 - \frac{\sigma_{br}}{\sigma_{la} - \sigma_{la,0}}\right), \\ &\qquad (\sigma_{br} < \sigma_{la} - \sigma_{la,0}) \\ C_{ad,d} &= \frac{\sigma_{br}}{\sigma_{la} - \sigma_{la,0}}, \qquad (\sigma_{br} \geq \sigma_{la} - \sigma_{la,0}) \end{aligned}\right\} \tag{14}$$

$$\sigma_{la,0} = -\frac{2}{\pi} \frac{E_{la}}{E_{Al}} \cos^{-1}\left(\frac{\sin\dfrac{\pi s}{W}}{\sin\dfrac{\pi a}{W}}\right) \sigma_{r,Al} \tag{15}$$

$$h = F_{Al} \sqrt{\frac{1}{jF_{ad} F_{Al}} + \frac{1}{jF_{ad} F_{gl}}} \tag{16}$$

$$F_{Al} = E_{Al} t_{Al}, \quad F_{ad} = \frac{G_{ad}}{t_{ad}} \tag{17}$$

$$\sigma_{br} = 2 \frac{C_{fW2}}{C_{fW1}} \frac{F_{gl}}{t_{la} E_{Al}} \frac{\sqrt{a^2 - s^2}}{b_s} C_d (\sigma_{Al} - \sigma_{Al,0}). \tag{18}$$

The notations used in ΔK_{fin} and the values of the notations substituted in the present study are as follows:

- s Half notch length, 1.5 mm
- σ_{la} Remote stress in GLARE
- E_{la} Young's modulus of GLARE3-5/4, 58 GPa
- t_{la} Total thickness of GLARE3-5/4, 2.6 mm
- E_{Al} Young's modulus of 2024-T3 aluminum alloy, 74 GPa
- t_{Al} Total thickness of the 2024-T3 aluminum alloy sheets, 1.51 mm
- E_{gl} Young's modulus of glass/adhesive layers, 35 GPa

$$E_{gl} = \frac{(E_{la} - E_{Al}) t_{Al} + E_{la} t_{gl}}{t_{gl}}$$

- t_{gl} Total thickness of glass/adhesive layers, 1.01 mm
- G_{ad} Shear modulus of adhesive, 0.64 GPa
- t_{ad} Total thickness of the adhesive, 0.027 mm

The da/dN—ΔK relationship for a GLARE using ΔK_{fin} has not been published to date. The stress intensity factor range ΔK_{fin} is given by:

$$\Delta K_{fin} = (K_{fin})_{\max} - (K_{fin})_{\min}. \tag{19}$$

The relationship between the delamination size and crack length was obtained by measuring the delamination using an ultrasonic C-scanner.

The delamination area was determined according to the following procedures:

(1) The fatigue test was suspended at an almost constant interval, and the specimen was removed from the testing machine.
(2) Ultrasonic C-scan pictures around the crack were taken.
(3) The specimen was installed in the testing machine again and the fatigue test was continued.

The above procedures (1) to (3) were repeated to determine the relationship between crack length and delamination size. Figures 13(a) ～ (c) indicate examples of ultrasonic C-scan pictures at a crack length of 12, 20, and 30 mm at the maximum stress level of 147 MPa. The light-gray part around the crack is considered to be a delamination area, and this shape is approximately an ellipse except for the vicinity of the crack tips.

The validity of the ultrasonic measurement was examined as follows. The surface aluminum alloy sheet of the specimen at a crack length of 30 mm was gradually removed using an end mill tool. The part of the aluminum alloy sheet that was swelling out of plane was removed, and an internal glass fiber layer was exposed as shown in Figure 14. The shape of the removed aluminum alloy approximately corresponded to the shape of the delamination area revealed by the ultrasonic picture. An identical result was found in other cases also. Therefore, the delamination measurement in this study is considered appropriate. The delamination width, b_s, defined in Figure 15 was determined. The b_s—a relationship is presented in Figure 16. Each solid line is drawn by the third-order polynomial approximation. The arrows correspond to those in Figure 11. The size of b_s increases as crack length and maximum stress increase.

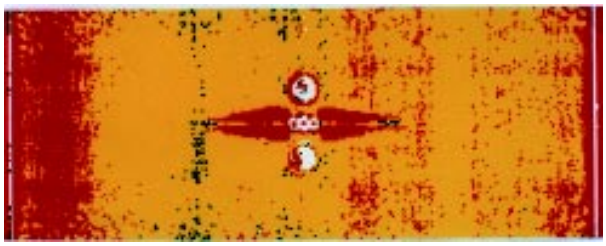

(a) $a \sim 12$ mm

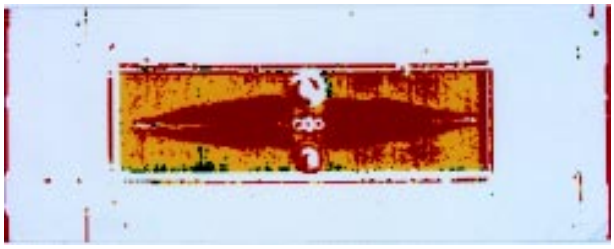

(b) $a \sim 20$ mm

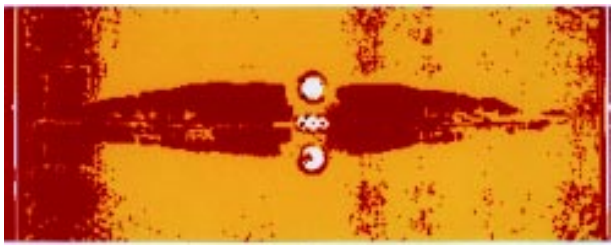

(c) $a \sim 30$ mm

Fig. 13 Ultrasonic C-scan pictures of the delamination in the GLARE3-5/4 under constant amplitude loading of $\sigma_{max} = 147$ MPa.

Fig. 14 Removal of the region swelling out of the plane in the GLARE3-5/4 at a 30 mm under constant amplitude loading of $\sigma_{max} = 147$ MPa.

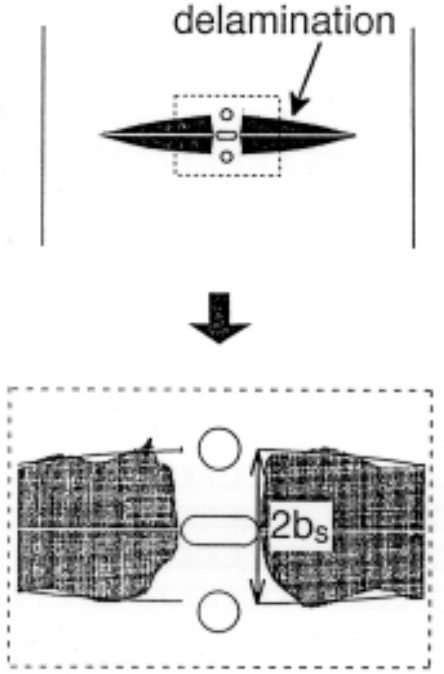

Fig. 15 Schematic view of delamination around a fatigue crack and definition of the delamination width b_s.

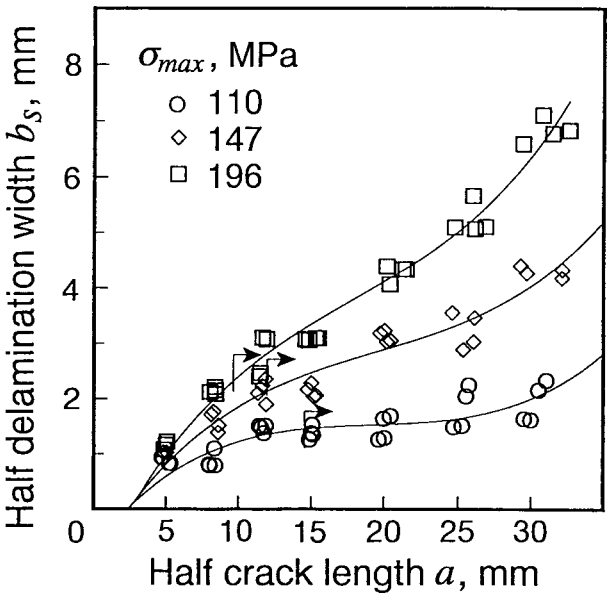

Fig. 16 Influence of the maximum stress level on the relationship between delamination width and crack length.

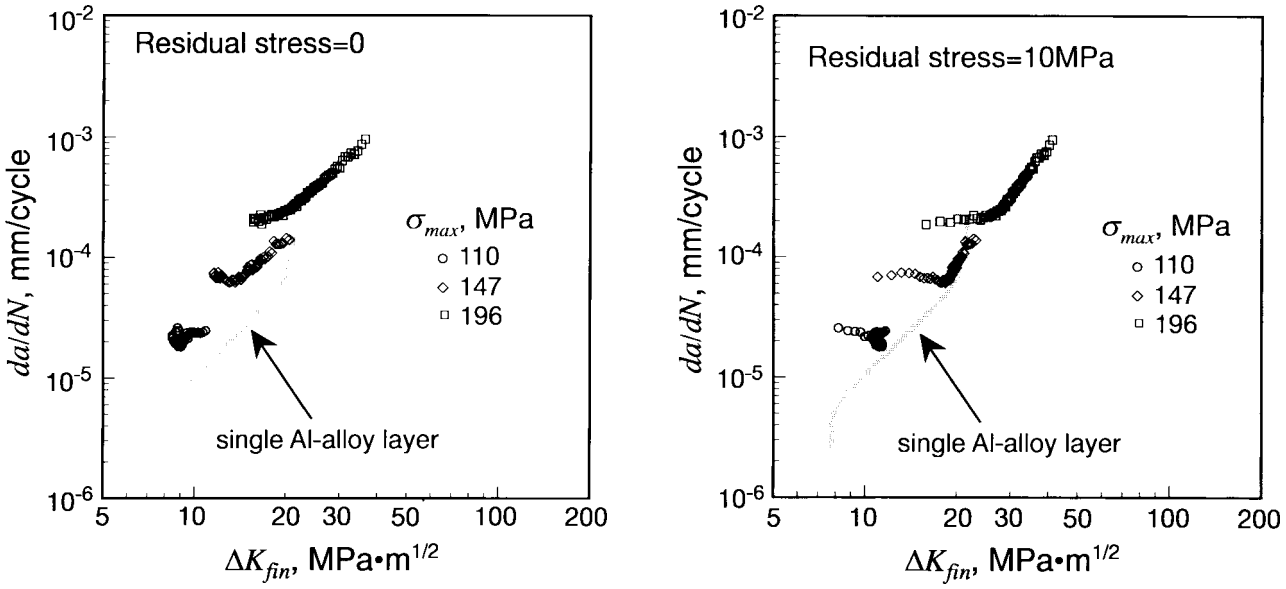

(a) A residual stress not considered (b) A residual stress of 10 MPa considered

Fig. 17 Relationship between da/dN and ΔK_{fin} in the GLARE 3-5/4 on the basis of Marissen 's formula.

Figure 17(a) presents the da/dN—ΔK_{fin} relationship by using ΔK_{fin} and the approximation of the b_s—a relationship shown in Figure 16 without considering residual stress. The bold curve indicates the da/dN—ΔK relationship for a single sheet specimen of the aluminum alloy. In comparison with ΔK in Figure 11, Figure 17(a) reveals that ΔK_{fin} is generally smaller than ΔK. In addition, the da/dN—ΔK_{fin} relationship is fairly close to the da/dN—ΔK relationship for the aluminum alloy independent of the maximum stress level. Consequently, the validity of Marissen 's formula for the GLARE3-5/4 is virtually confirmed. However, the da/dN—ΔK_{fin} relationship deviates slightly from the straight part of the da/dN—ΔK relationship for the aluminum alloy. The reasons for this result are considered to be as follows.

(1) The residual stresses in an aluminum alloy sheet were not considered in the calculation of ΔK_{fin} in Figure 17(a).

(2) Marissen assumed the shape of the delamination to be an ellipse. However, the shape of the delamination in this study was not exactly an ellipse as shown in Figure 13.

Various values of the tensile residual stress were assumed, and the influence of the residual stress on the da/dN—ΔK_{fin} relationship was examined. If the tensile residual stress was assumed to be about 10 MPa, the da/dN—ΔK_{fin} relationship for the GLARE3-5/4 would most closely approach the da/dN—ΔK relationship for a single sheet specimen of the aluminum alloy as illustrated in Figure 17(b).

The residual stress was evaluated using the following equation (20) to examine the validity of the above presumed value. The equation is obtained on the assumption that the residual stress is caused by the difference of the coefficient of thermal expansion between 2024-T3 aluminum alloy sheets and fiber-adhesive layers.

$$\sigma_i = \frac{E_{Al}E_{gl}(\gamma_{Al}-\gamma_{gl})\,\Delta T}{E_{Al}(1-\gamma_{gl}\Delta T)+E_{gl}(1-\gamma_{Al}\Delta T)} \qquad (20)$$

where E_{Al} and E_{gl} is Young 's modulus, γ_{Al} and γ_{gl} are the coefficient of thermal expansion for 2024-T3 aluminum alloy sheets and glass fiber-adhesive layers respectively, and ΔT is the difference between the curing temperature of the epoxy resin and room temperature. Substituting $E_{Al} = 74$ GPa, $E_{gl} = 34.5$ GPa, $\gamma_{Al} = 21.6 \times 10^{-6}$/°C[16], $\gamma_{gl} = 7 \sim 11 \times 10^{-6}$/°C[7], and $\Delta T \simeq 100$ °C (estimated from curing temperature $\simeq 120$ °C[6]) in Eq. (20), the resultant σ_i was calculated to be 25 ~ 35 MPa in tension. These values of σ_i do not agree with the assumed value of 10 MPa. However, the order of this value is confirmed, though further investigations will be necessary. The difference of 15 ~ 25 MPa may originate from the existence of the stress gradient caused by the interface resin between the aluminum alloy sheets and

the 0° glass fibers.

CONCLUSIONS

The scatter and properties of fatigue crack growth of a GLARE3-5/4 fiber/metal laminate were investigated by fatigue tests under constant amplitude loading. The data of fatigue crack growth were analyzed by Toi's simple model and the stress intensity factor formula provided by Marissen to evaluate both analytical methods. The major conclusions obtained are as follows:

1. The coefficient of variation of fatigue crack growth of the GLARE3-5/4 was calculated to be 8 to 9 % by the test results for 11 specimens and about twice higher than that of a 2024-T3 aluminum alloy obtained by 18 specimens in the previous studies[13],[14].
2. The relationship between crack growth rate, da/dN, and stress intensity factor range, ΔK, of the GLARE3-5/4 obtained on the assumption of a monolithic material was dependent on the maximum stress level and was different from that for a single-sheet specimen of the 2024-T3 aluminum alloy machined from a GLARE3-5/4 specimen.
3. The da/dN—ΔK relationship was divided into two regions, and da/dN varied from decreasing to increasing at a certain ΔK as crack length increased at a small maximum stress level. da/dN at a large maximum stress level generally increased.
4. The modified factor proposed by Toi as a function of fatigue crack length was dependent on the maximum stress level and was not generally applicable.
5. On the basis of the formula of ΔK_{fin} provided by Marissen, the measured delamination, and an assumed residual stress of 10 MPa, the da/dN versus ΔK_{fin} relationship for the GLARE3-5/4 approximately agreed with that of a single sheet of 2024-T3 aluminum alloy independent of the maximum stress level.
6. The order of the assumed residual stress in Marissen's formula was confirmed by a rough estimation.

ACKNOWLEDGMENTS

The authors wish to thank Mr. Toi of Fuji Heavy Industries Co., Ltd., for his kind advice.

REFERENCES

[1] L.B. Vogelesang, R. Marissen, and J. Schijve, "A new fatigue resistant material : aramid reinforced aluminum laminate (ARALL)," *Proceedings of the 11th ICAF Symposium*, (1981), Noordwijkerhout, NLR, 3.4/1-3.4/39.

[2] J. Schijve, "Fatigue of aircraft materials and structures," Fatigue of Aircraft Materials, eds. A. Beukers et al., Delft University Press, (1992), 113-140.

[3] J. Schijve, "Development of fiber-metal laminate, ARALL and GLARE, new fatigue resistant materials," *Report LR-715*, Faculty of Aerospace Eng., Delft University of Technology, (1993).

[4] J.B. Young, J.G.N. Landry, and V.N. Cavoulacos, "Crack growth and residual strength characteristics of two grades of glass-reinforced aluminum 'Glare'," *Composite Structures*, 27 (1994), 457-469.

[5] Y. Toi, "An experimental crack growth model for fiber/metal laminates," *Proc. 18th Symposium of ICAF*, Melbourne, (1995), 899-909.

[6] T. Miyata, T. Tagawa, F. Takahashi, and H. Hira, "Fatigue crack propagation behavior of fiber metal laminate — influence of initial notch length and pre-stretching—," *J. Soc. Mat. Sci., Japan*, 45-3 (1996), 334-339 (in Japanese).

[7] R. Marissen, "Flight simulation behavior of aramid reinforced aluminum laminates (ARALL)," *Eng. Frac. Mech.*, 19-2 (1984), 261-277.

[8] R. Marissen, "Fatigue crack growth in ARALL. A hybrid aluminum-aramid composite material, crack growth mechanics and quantitative predictions of the crack growth rate," *Report LR-574*, Faculty of Aerospace Eng., Delft University of Technology, (1988).

[9] R.O. Ritchie, Weikang Yu, and R.J. Bucci, "Fatigue crack propagation in ARALL laminates ; Measurement of the effect of crack-tip shielding from crack bridging," *Eng. Frac. Mech.*, 32-3 (1989), 361-377.

[10] J. Macheret, J.L. Teply, and E.F.M. Winter, "Delamination shape effects in aramid-epoxy-aluminum (ARALL) laminates with fatigue

cracks," *Polymer Composites*, 10-5 (1989), 322-327.

[11] D.L. Davidson and L.K. Austin, "Fatigue crack growth through ARALL-4 at ambient temperature," *Fatigue & Fracture of Eng. Materials & Structures*, 14-10 (1991), 939-951.

[12] C.T. Lin, P.W. Kao, and F.S. Yang, "Fatigue behavior of carbon fiber-reinforced aluminum laminates," *Composites*, 22-2 (1991), 135-141.

[13] M. Ichikawa, S. Akita, T. Takamatsu, T. Matsumura, M. Satoh, and S. Nishijima, "Reliability engineering approach to fatigue crack growth rate using DC electrical potential method," *J. Soc. Mat. Sci., Japan*, 37-420 (1988), 1010-1016 (in Japanese).

[14] M. Ichikawa, T. Takamatsu, T. Matsumura, N. Suzuki, and S. Nishijima, "Statistical experiment on fatigue crack growth rate using DC electrical potential method and examination of stochastic models (2024-T3 Al Alloy)," *J. Soc. Mat. Sci., Japan*, 40-450 (1991), 283-288 (in Japanese).

[15] D.A. Virkler, B.M. Hillberry, and P.K. Goel, "The statistical nature of fatigue crack propagation," *Trans. ASME, J. of Eng. Materials and Technology*, 101 (1979), 148-153.

[16] Science chronological tables, ed. National Astronomical Observatory, Maruzen, Tokyo, (1996), 485 (in Japanese).

[17] *Plastic composite materials*, Nikkan Kogyo Shinbun, Tokyo, (1984), 41 (in Japanese).